Dipeptidyl peptidase IV inhibitor protects against renal interstitial fibrosis in a mouse model of ureteral obstruction

Hye Sook Min[1], Jung Eun Kim[1], Mi Hwa Lee[1], Hye Kyoung Song[1], Young Sun Kang[1], Mi Jin Lee[1], Ji Eun Lee[2], Hyun Wook Kim[2], Jin Joo Cha[1], Young Yoon Chung[1], Young Youl Hyun[3], Jee Young Han[4] and Dae Ryong Cha[1]

Dipeptidyl peptidase IV (DPPIV) is an exopeptidase that modulates the function of several substrates, among which insulin-releasing incretin hormones are the most well known. DPPIV also modulate substrates involved in inflammation, cell migration, and cell differentiation. Although DPPIV is highly expressed in proximal renal tubular cells, the role of DPPIV inhibition in renal disease is not fully understood. For this reason, we investigated the effects of LC15-0444, a DPPIV inhibitor, on renal function in a mouse model of renal fibrosis. Eight-week-old C57/BL6 mice were subjected to unilateral ureteral obstruction (UUO) and were treated with LC15-0444 (a DPPIV inhibitor) at a dose of 150 mg/kg per day in food or vehicle for 14 days. DPPIV activity was significantly increased in obstructed kidneys, and reduced after treatment with LC15-0444. Administration of LC15-0444 resulted in a significant decrease in albuminuria, urinary excretion of 8-iso-prostane, and renal fibrosis. DPPIV inhibition also substantially decreased the synthesis of several proinflammatory and profibrotic molecules, as well as the infiltration of macrophages. UUO significantly increased, and LC15-0444 markedly suppressed, levels of phosphorylated Smad2/3, TGFβ1, toll-like receptor 4, high-mobility group box-1, NADPH oxidase 4, and NF-κB. These results suggest that activation of DPPIV in the kidney has a role in the progression of renal disease and that targeted therapy inhibiting DPPIV may prove to be a useful new approach in the management of progressive renal disease, independent of mechanisms mediated by glucagon-like peptide-1.

Glucagon-like peptide-1 (GLP-1) and gastrointestinal peptide (GIP) are incretin hormones that lower serum glucose. Their half-lives are short because dipeptidyl peptidase 4 (DPPIV) rapidly converts bioactive GLP-1 and GIP to their inactive metabolites.[1,2] DPPIV is a serine protease that cleaves off N-terminal dipeptides from peptide substrates.[3] DPPIV inhibitor lowers serum glucose by inhibiting the degradation of incretin hormones, and then induces some of the similar effects of incretin hormones such as activation of insulin secretion, inhibition of glucagon secretion, and improvement of β-cell mass.[3] For this reason, several DPPIV inhibitors (sitagliptin, vildagliptin, saxagliptin, and linagliptin) are used in the treatment of type 2 diabetes mellitus.[3]

DPPIV is a so-called 'moonlighting protein' with a variety of functions that vary depending on intracellular *vs* extracellular location, cell type, oligomeric *vs* polymeric state, and concentrations of ligand, cofactor, or product.[4,5] DPPIV has been found to function as a serine protease, a receptor, a costimulatory protein, and as an adhesion molecule for collagen and fibronectin, as well as having roles in apoptosis and immune regulation.[6] It has been found to have roles in several important diseases, including melanoma, autoimmune diseases, and AIDS.[6]

DPPIV acts on a wide variety of substrates involved in metabolism, glucose regulation, inflammation, cell migration, and cell differentiation.[7] Certain substrates of DPPIV,

[1]Division of Nephrology, Department of Internal Medicine, Korea University Ansan-Hospital, Korea University, Ansan, Korea; [2]Division of Nephrology, Department of Internal Medicine, Wonkwang University, Gunpo, Korea; [3]Division of Nephrology, Department of Internal Medicine, Sungkyunkwan University, Seoul, Korea and [4]Department of Pathology, Inha University, Incheon, Korea

Correspondence: Professor DR Cha, MD, Division of Nephrology, Department of Internal Medicine, Korea University Ansan-Hospital, Korea University, 516 Kojan-Dong, Ansan, Kyungki-Do 425-020, Korea.
E-mail: cdragn@unitel.co.kr

including BNP/ANP, NPY, PYY, and SDF-1α, have been found to affect the renal and cardiovascular systems.[8] Recently, investigations of DPPIV have focused on identifying new physiologically relevant substrates, such as RANTES, neuropeptide Y, and substance P.[9,10] High-mobility group box-1 (HMGB-1) protein is a cytokine identified in 2012 as a substrate of DPPIV that mediates responses to infection, injury, and inflammation.[11,12] A 2012 paper proposed HMGB-1 as a causative factor in renal damage.[13] DPPIV has high expression levels and activity in the kidney, and is found on the apical/brush border surface of proximal renal tubular cells and in the urine.[14] However, the roles of DPPIV and its inhibition are not fully understood in the pathogenesis of renal disease. For this reason, we investigated the roles of DPPIV and its inhibition on renal function in a mouse model of renal fibrosis.

MATERIALS AND METHODS
Animal Studies
We divided 8-week-old C57/BL6 mice into four groups: sham treatment alone ($N = 6$), sham treatment with LC15-0444, a DPPIV inhibitor ($n = 5$), unilateral ureteral obstruction (UUO) with vehicle ($N = 7$), and UUO treated with LC15-0444 ($N = 7$). UUO was performed by complete ligation of the left ureters with 6-0 silk at two points and a cut was made between them. The upper ligation was consistently placed at the level of the lower pole of the kidney. After causing UUO, mice were fed with either normal chow or chow mixed with 150 mg/kg per day of LC15-0444 for 14 days. All mice were provided with a standard diet and water, and were maintained at constant temperature ($23 \pm 2\,^\circ$C) and humidity (55 ± 5%) with a 12-h light/dark cycle. Daily food intake was monitored at regular intervals to confirm drug administration. At the end of the study period, systolic blood pressure was measured using tail-cuff plethysmography (LE 5001-Pressure Meter; Letica SA, Barcelona, Spain). Plasma creatinine levels were determined by a modified Jaffe method. Plasma triglyceride, cholesterol, HDL-C and LDL-C analyses were performed using a commercial kit (Wako Chemicals, Richmond, VA, USA). To determine urinary albumin excretion, mice were caged individually and 24-h urine was collected. Urinary albumin concentrations were determined by competitive enzyme-linked immunosorbent assay (ELISA) kit (ALPCO, Westlake, OH, USA). Plasma and urine 8-isoprostane levels were measured using an ELISA kit (Cayman Chemical, Ann Arbor, MI, USA). Plasma active GLP-1 levels were determined by ELISA kit (Millipore, St Charles, MO, USA). Mice were killed under anesthesia with intraperitoneal injections of sodium pentobarbital (50 mg/kg). All the samples were analyzed by ELISA in triplicate, and the results were averaged. All experiments were conducted in accordance with National Institutes of Health guidelines and with the approval of the Korea University Institutional Animal Care and Use Committee.

Assay for DPPIV Activity
DPPIV activity in plasma, cell and tissues was measured as described previously.[15] Briefly, 0–40 μM of AMC (7-amino-4-methylcoumarin) standard was loaded into each well individually and fluorometric measurements were taken at Em/Ex = 360/465 nm, generating a linear standard curve. Next, 50 μl of plasma sample was added to each of 96 wells, followed by the addition of 50 μl substrate solution (0.1 M HEPES, 50 μM Gly-Pro-AMC, and 50 μg BSA) per well. Plates were immediately measured using a Spectramax GEMINI XPS fluorescence microplate reader (Molecular Devices, Sunnyvale, CA, USA; Em/Ex = 360/465 nm, kinetic interval = 25 s, number of kinetic cycles = 12, target temperature = 25 $^\circ$C, incubation time = 0 s). To analyze DPPIV activity in renal tissues and cells, frozen tissues (10 mg) or cells (2×10^6) were homogenized in cold assay buffer (25 mM Tris-HCl, 140 mM NaCl, 10 mM KCl, pH 7.5, 0.1% BSA) and centrifuged at 20 000 g for 20 min at 4 $^\circ$C. DPPIV activity was measured in the lysate using the fluorogenic substrate H-GlyPro-AMC. DPPIV activity in each tissue was expressed as the amount of cleaved AMC per minute per tissue weight (μM/min per g tissue). DPPIV activity assay was tested in all samples in duplicates, and the results were averaged.

Analysis of Gene Expression by Real-Time Quantitative PCR in Tissues and Cells
Total RNA was extracted from renal cortical tissues and cells with Trizol reagent and further purified using an RNeasy Mini kit (Qiagen, Valencia, CA, USA). The nucleotide sequences of all primers used in this study are shown in Supplementary Table 1. Quantitative gene expression was performed on a LightCycler® 1.5 system (Roche Diagnostics Corporation, Indianapolis, IN, USA) using SYBR Green technology. Real-time RT-PCR was performed for 10 minutes at 50 $^\circ$C and 5 minutes at 95 $^\circ$C, followed by 22–30 cycles of denaturation for 10 s at 95 $^\circ$C and annealing with extension for 30 s at 60 $^\circ$C. The ratios of each gene and β-actin level (relative gene expression number) were calculated by subtracting the threshold cycle number (Ct) of the target gene from that of β-actin and raising 2 to the power of this difference.

Protein Extraction and Western Blot Analysis
Nuclear and cytoplasmic proteins were extracted from renal cortical tissues and cells using a commercial nuclear extraction kit (Active Motif, Carlsbad, CA, USA). For western blotting, 40 μg protein was electrophoresed on a 10% SDS-PAGE minigel. Proteins were transferred onto a polyvinylidene difluoride membrane, and the membrane was hybridized in blocking buffer overnight at 4 $^\circ$C with mouse monoclonal anti-NF-κB p65 antibody (1:1000; Cell Signaling Technology, Danvers, MA, USA), rabbit polyclonal anti-TGFβ1 antibody (1:200; Santa Cruz Biotechnology, Santa Cruz, CA, USA), rabbit polyclonal phospho-specific ERK1/2, total ERK1/2 (1:1000; Cell Signaling Technology, Danvers, MA, USA), goat polyclonal anti-toll-like receptor 4

(TLR4) antibody (1:500; Santa Cruz Biotechnology), rabbit polyclonal anti-NADPH oxidase 4 (NOX4) antibody (1:500; Novus Biologicals, Littleton, CO, USA), goat polyclonal phosphospecific-anti-Smad2/3, total Samd2/3 antibody (1:100; Santa Cruz Biotechnology), rabbit polyclonal anti-HMGB1 antibody (1:100; Abcam Plc, Cambridge, MA, USA), rabbit polyclonal anti-GLP1 receptor antibody (1:100; Abcam Plc), rabbit polyclonal anti-DPPIV (CD26) antibody (1:2000; Abcam Plc), mouse monoclonal anti-β-actin antibody (1:5000; Sigma-Aldrich) or mouse monoclonal anti-TATA-binding protein (TBP) antibody (1:1000; Abcam Plc). The membrane was subsequently incubated with horseradish peroxidase-conjugated secondary antibody (1:1000 dilution) for 60 min at room temperature. Specific signals were detected using the enhanced chemiluminescence method (Amersham, Buckinghamshire, UK).

Light Microscopy and Immunohistochemistry

Kidney samples were fixed in 10% buffered formalin and embedded in paraffin. Kidney tissue was cut into 4-μm-thick slices and stained with periodic acid Schiff (PAS), Masson's trichrome and sirius red staining. After Masson's trichrome staining, the degree of tubulointerstitial fibrosis was assessed by a point-counting method as described previously.[16] Briefly, a standardized grid of 70 points was superimposed on the microscope, and the number of points over the glomeruli, tubular epithelium, and interstitial tissue were counted and scored as 0 for 0%, 1 for <25%, 2 for 25–50%, 3 for 51–75%, and 4 for >75% for each field with tubulointerstitial fibrosis. Macrophage infiltration was detected by rat anti-mouse F4/80 antibody (1:2000; Serotec, Raleigh, NC, USA) and incubated at room temperature for 1 h, followed by use of the Envision kit (Dako, Carpinteria, CA, USA). Macrophages infiltrating the interstitium were counted and expressed as the number of macrophages per high-power field. To perform immunohistochemical staining for type I collagen, TGFβ1, and α-SMA, kidney sections were transferred to a 10 mmol/l citrate buffer solution adjusted to a pH of 6.0. Thereafter, sections were microwaved for 10–20 min to retrieve antigens for TGFβ1 and α-SMA, or treated with trypsin (Sigma, St Louis, MO, USA) for 30 min at 37 °C for type I collagen. To block endogenous peroxidase activity, 3.0% H_2O_2 in methanol was applied for 20 min, followed by incubation at room temperature for 60 min with 3% BSA/3% normal goat serum. Slides were incubated overnight at 4 °C with rabbit polyclonal anti-TGFβ1 antibody and rabbit polyclonal anti-type I collagen antibody (1:200; Santa Cruz Biotechnology), and rabbit polyclonal anti-α-SMA antibody (1:100; Santa Cruz Biotechnology). For coloration, slides were incubated at room temperature with a mixture of 0.05% 3,3'-diaminobenzidine containing 0.01% H_2O_2 and then counterstained with Mayer's hematoxylin. Negative control sections were stained under identical conditions with a buffer solution that was substituted for the primary antibody.

A pathologist carried out the histological examinations in a blinded manner.

In Vitro Experiment

In this experiment, we used a mouse podocyte cell line that was obtained from Peter Mundel at the Albert Einstein College of Medicine (New York, NY, USA). Mouse mesangial cells were obtained from a portion of the renal cortex from normal C57BL/6 mice using the differential sieving method. Rat proximal tubule cells (NRK-52E) were purchased from American Type Culture Collection (ATCC, Rockville, MD, USA). Experimental cells were cultured in DMEM supplemented with 10% FCS and 100 μg/ml of penicillin/streptomycin. To evaluate the basal expression levels of DPPIV, subconfluent cells were serum-starved for 24 h, and harvested to determine RNA and protein expression. As most DPPIV expression was profoundly observed in PTC, we next performed another experiment using PTC. Because TGFβ1 is one of the most important mediators of renal fibrosis in UUO, we next evaluated the effect of TGFβ1 on DPPIV activity. Subconfluent PTCs were cultivated with or without TGFβ1 at a final concentration of 10 ng/ml for 24 h, and the harvested for the measurement of DPPIV activity. All experimental groups were cultured in triplicate.

Statistical Analysis

Nonparametric analysis was used because of the small sample size. Results are expressed as mean ± s.e.m. Multiple comparisons were carried out using Wilcoxon's rank-sum tests and Bonferroni correction. A Kruskal–Wallis test was used to compare more than two groups, followed by a Mann–Whitney *U*-test, using a microcomputer-assisted program called SPSS for Windows 12.0 (SPSS, Chicago, IL, USA). A *P*-value <0.05 was considered statistically significant.

RESULTS

Effects of LC15-0444 on Biochemical and Physical Parameters in Experimental Animals

Table 1 shows biochemical results for each group. Body weight and kidney weight were significantly lower in the UUO group than in the sham operation group and the sham group treated with LC15-0444. There were no significant differences in urine volume, plasma creatinine levels, or plasma lipid levels. Systolic blood pressure was significantly higher in the UUO group than in the sham group and the sham group treated with LC15-0444. However, LC15-0444 treatment did not induce any significant changes in systolic blood pressure.

Effects of LC15-0444 on DPPIV Activity, Plasma 8-Isoprostane, and Urinary Excretion of Protein, Albumin and 8-Isoprostane

Although plasma DPPIV activity tended to be lower in mice treated with LC15-0444, there was no significant difference among the four groups because of large interindividual

Table 1 Physical and biochemical parameters of experimental animals

Parameters	Control (sham)	Sham + LC15-0444	UUO	UUO + LC15-0444
Urine volume(ml per day)	0.25 ± 0.05	0.34 ± 0.10	0.36 ± 0.07	0.39 ± 0.04
Body weight (g)	23.1 ± 0.55	22.7 ± 0.40	20.9 ± 0.38**	21.4 ± 0.50*
Kidney/100 g BW	1.40 ± 0.35	1.20 ± 0.07	0.89 ± 0.04***	0.88 ± 0.02***
P-creatinine (μmol/l)	35.0 ± 4.0	40.0 ± 4.0	44.0 ± 4.0	27.0 ± 4.0
Cholesterol (mg/dl)	56.6 ± 2.10	47.5 ± 4.12	60.0 ± 4.36	54.0 ± 4.85
Triglyceride (mg/dl)	55.0 ± 12.3	53.7 ± 7.2	30.0 ± 4.36	37.1 ± 6.06
HDL-cholesterol (mg/dl)	76.0 ± 2.73	67.0 ± 7.11	68.0 ± 7.03	67.4 ± 7.16
LDL-cholesterol (mg/dl)	22.0 ± 3.2	21.3 ± 4.5	29.8 ± 2.1	26.7 ± 2.2
Active GLP-1 (pM)	1.94 ± 0.27	2.21 ± 0.36	2.12 ± 0.35	2.31 ± 0.39
SBP (mm Hg)	121 ± 2	118 ± 5	136 ± 3***	137 ± 2***

Abbreviation: P, plasma.
Values are expressed as means ± s.e.m. *$P<0.05$; **$P<0.01$; ***$P<0.001$ *vs* sham and sham + LC15-0444.

variation (Figure 1a). Renal DPPIV activity was significantly increased in mice that underwent UUO; those treated with LC15-0444 had markedly suppressed DPPIV activity (Figure 1b). Even in the control sham group, LC15-0444 treatment significantly suppressed renal DPPIV activity (Figure 1b). In addition, urinary levels of 8-isoprostane, which reflect oxidative stress in the kidney, were markedly increased after UUO, but significantly decreased in mice treated with LC15-0444 (Figure 1c). However, LC15-0444 treatment did not show significant difference in urinary excretion of 8-isoprostane in the control sham group (Figure 1d). As LC15-0444 treatment may decrease systemic levels of oxidative stress, we next measured plasma levels of 8-isoprostane. As shown in Figure 2a, there was no significant difference in the plasma concentration of 8-isoprostane among four groups. In accordance with these changes, urinary excretion of albumin was markedly increased after UUO, and significantly decreased after LC15-0444 treatment (Figure 2b). However, there was no significant difference in microalbuminuria in the sham group with or without treatment with LC15-0444 (Figure 2b).

Effects of LC15-0444 on Renal Structural Changes

Figure 3 show representative renal pathology and immunostaining for F4/80 and α-SMA in treated and untreated mice. PAS and Masson's trichrome staining revealed extensive tubulointerstitial damage, including interstitial fibrosis and tubular atrophy, in untreated mice with UUO. In fact, this group exhibited enhanced fibrosis as demonstrated by increased collagen I, TGFβ1, and α-SMA accumulation in the fibrotic area of the tubulointerstitium (Figure 3, Supplementary Figure 1). We used F4/80 staining to examine renal

macrophage infiltration as a marker of inflammation, a critical result of UUO. As shown in Figure 3, there was significant macrophage infiltration in the tubulointerstitium after UUO. Mice treated with LC15-0444 exhibited less extensive interstitial fibrosis, tubular atrophy, α-SMA expression, and macrophage infiltration (Figure 3). However, LC15-0444 treatment did not show significant structural changes and macrophage infiltration in the sham group. Compared with the obstructed kidney, there was no tubulointerstitial damage but macrophage infiltration showed severe changes in the contralateral unobstructed kidney. However, these changes were more evident in the untreated UUO group, and LC15-0444 treatment significantly suppressed renal inflammation in the contralateral unobstructed kidney in the UUO group (Figure 3 and Supplementary Figure 1). In accordance with this morphological alteration, mRNA expression levels of proinflammatory cytokines were remarkably upregulated in both obstructed and contralateral unobstructed kidney in the UUO group, and LC15-0444 treatment also decreased renal expression of proinflammatory and profibrotic molecules such as MCP-1, PAI-1, TGFβ1, type I collagen, and TNFα (Figures 4a and b). Furthermore, quantitative analysis with immunohistochemical staining showed similar results (Figures 4c and d).

Effects of LC15-0444 on Oxidative Stress and Inflammatory Molecules

We next examined the inflammatory and fibrotic signaling cascades in mice that underwent UUO. As shown in Figure 5, western blot analysis showed significant upregulation of inflammatory molecules, including toll-like receptor 4, NOX4 and NF-κB (p65) protein, as well as fibrotic molecules, including TGFβ1 and p-Smad2/3, in the obstructed kidney. All of these molecules were decreased in mice treated with LC15-0444. Although these changes were less severe in the contralateral unobstructed kidney compared with those in obstructed kidney in UUO group, inflammatory molecules were still significantly upregulated compared with control sham kidney. In addition, LC15-0444 significantly downregulated inflammatory molecules in the contralateral unobstructed kidney. However, LC15-0444 treatment did not show significant changes in the control sham group. Of note, the obstructed kidneys showed no significant change in ERK activation, but decreased expression of the GLP-1 receptor, neither of which was affected by LC15-0444 treatment. The expression of HMGB1, an inflammatory mediator, was not upregulated in mice with UUO, but was in fact suppressed in mice treated with LC15-0444.

Basal DPPIV Activity in Intrinsic Renal Cells and Effects of TGFβ1 Stimulation on DPPIV Activity in Cultured Proximal Tubular Cells

We next examined the DPPIV expression, which was significantly increased after UUO, in various renal cells. As shown in Figures 5a and b, basal DPPIV mRNA and protein
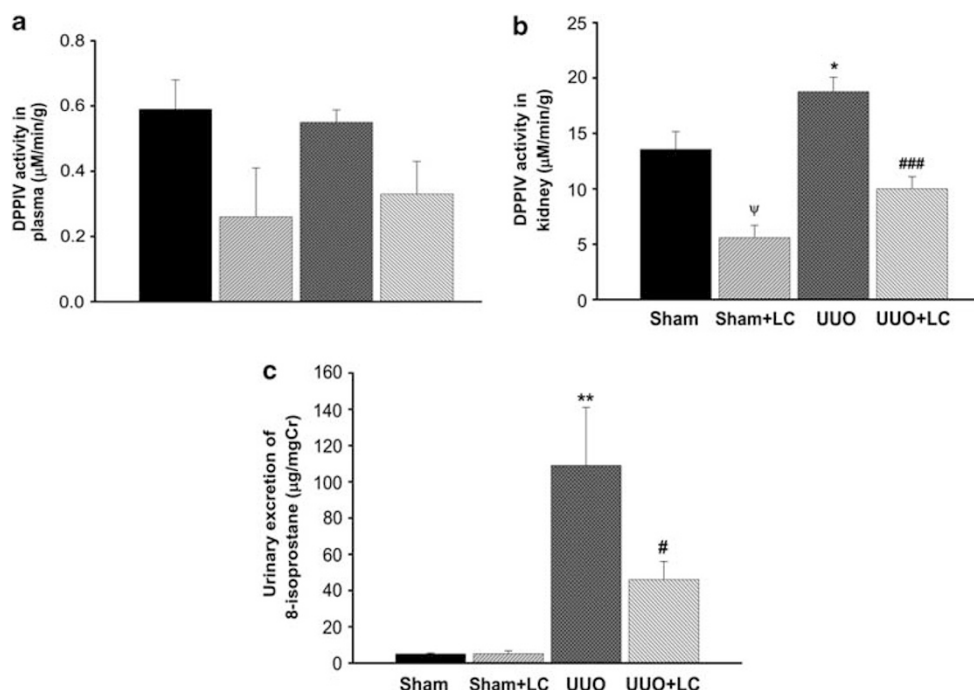
Figure 1 Effects of LC15-0444 (LC) on plasma and renal dipeptidyl peptidase IV (DPPIV) activity, and urinary excretion of protein and 8-isoprostane. (a) DPPIV activity in the plasma. (b) DPPIV activity in the kidney. (c) Twenty-four hour urinary level of 8-isoprostane. Urinary 8-isoprostane levels were corrected for urine creatinine levels. Data are expressed as mean ± s.e.m.; *$P < 0.05$, **$P < 0.01$, ***$P < 0.001$ vs sham and sham + LC; #$P < 0.05$, ###$P < 0.001$ vs unilateral ureteral obstruction (UUO); $^{\Psi}P < 0.001$ vs sham.
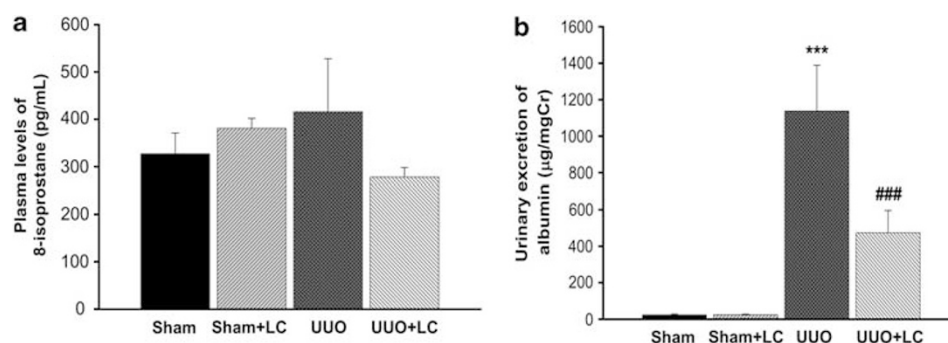

Figure 2 Effects of LC15-0444 (LC) on plasma 8-isoprostane levels and urinary excretion of microalbumin. (a) 8-Isoprostane concentration in the plasma. (b) Twenty-four hour urinary level of microalbumin. Urinary microalbumin levels were corrected for urine creatinine levels. Data are expressed as mean ± s.e.m.; ***$P < 0.001$ vs sham and sham + LC; ###$P < 0.001$ vs unilateral ureteral obstruction (UUO).

expression were most abundantly observed in proximal tubular cells (PTCs) compared with mesangial cells and podocytes. We also found that TGFβ1 stimulation, a major mediator in renal fibrosis, markedly increased DPPIV activity in PTCs (Figure 6c).

DISCUSSION

LC15-0444 is a selective and competitive inhibitor of DPPIV currently used in clinical practice for the treatment of type 2 diabetes.[17] The direct inhibition of DPPIV increases GLP-1 levels and improves the insulin response and glycemic control. In this study, we found that LC15-0444 decreased

urinary protein excretion and mitigated renal structural changes in obstructed and contralateral unobstructed kidneys. Our findings agree with those of previous studies, which demonstrated DPPIV inhibition to protect the kidney against ischemia–reperfusion injury animal models of type 1 and type 2 diabetic nephropathy.[18–21] It has been proposed that the protective effects of DPPIV inhibition are mediated by increased circulating levels of GLP-1.[17,20] In our study, we used a model of kidney injury to simulate progressive tubulointerstitial fibrosis and elucidate the effects of DPPIV inhibition independent of GLP-1. Plasma levels of GLP-1 did not differ significantly between groups. Furthermore, GLP-1
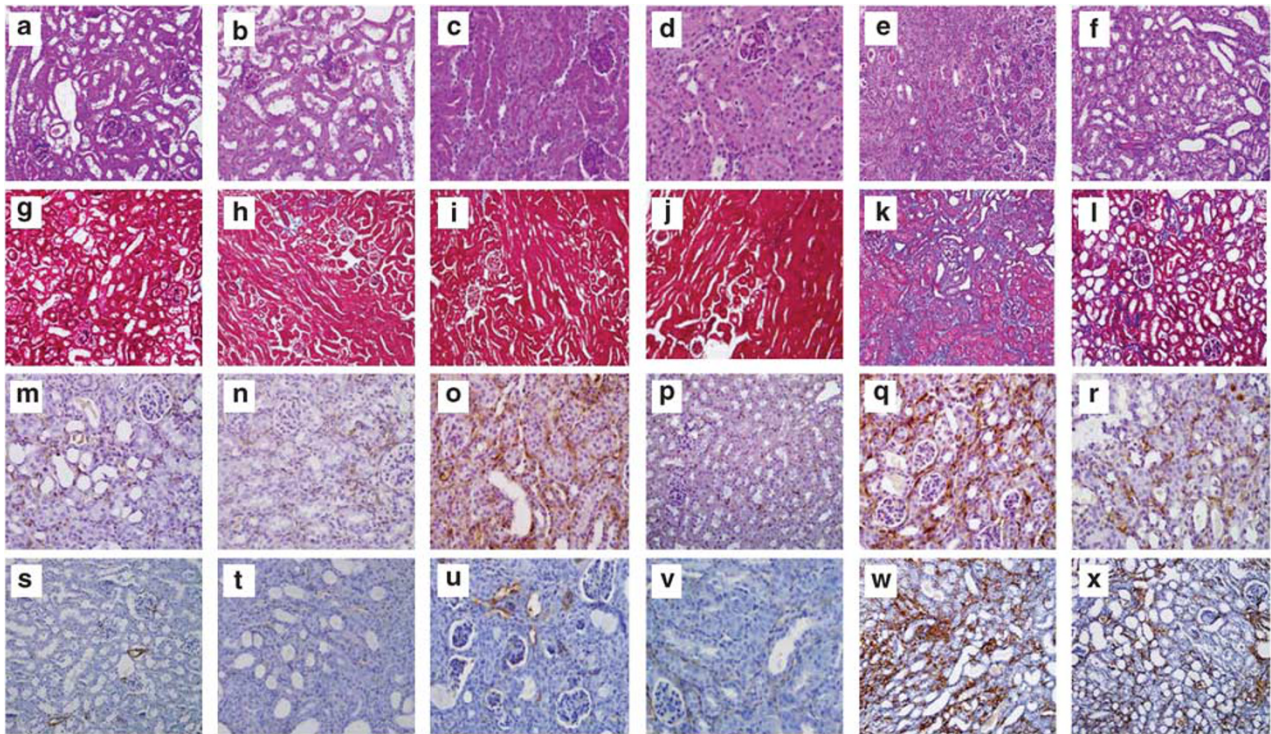
Figure 3 Representative renal histological and immunohistochemical staining in experimental models after 2 weeks of unilateral ureteral obstruction (UUO). (**a**, **g**, **m**, **s**) Sham-operation kidney; (**b**, **h**, **n**, **t**) sham + LC15-0444 (LC) kidney; (**c**, **i**, **o**, **u**) contralateral unobstructed kidney in UUO; (**d**, **j**, **p**, **v**) contralateral unobstructed kidney in UUO + LC; (**e**, **k**, **q**, **w**) obstructed UUO kidney; (**f**, **l**, **r**, **x**) obstructed kidney in UUO + LC. Representative periodic acid Schiff (PAS) staining (**a**–**f**), Masson's trichrome stain (**g**–**l**), F4/80 immunostaining (**m**–**r**), and α-smooth muscle actin (α-SMA) staining (**s**–**x**). Original magnification: ×400.

receptor expression was markedly decreased after UUO, and remained unchanged after LC15-0444 treatment. Our results suggest that the renoprotective effects of LC15-0444 are independent of GLP-1-mediated mechanisms.

LC15-0444, also known as gemigliptin (LG Life Sciences, Seoul, Republic of Korea), is a selective and competitive inhibitor of DPPIV and is currently used in clinical practice for the treatment of type 2 diabetic patients in Korea. In an animal experiment, LC15-0444 shows inhibition of DPPIV activity by ≥80%, which is associated with a maximal short-term lowering of glucose levels.[22] In addition, a twofold augmentation of postprandial active GLP-1 levels is associated with similar effects.[22] A phase I study conducted in healthy Korean male subjects after single administration of LC15-0444 at doses of either 25, 50, 100, 200, 400, or 600 mg found that a single dose of LC15-0444 exhibited linear PK properties over the range of 50–400 mg in study subjects.[23] In addition, PK characteristics were not significantly influenced by food, and doses ≥200 mg of LC15-0444 inhibited plasma DPP IV activity by >80% over a 24-h dosing interval, and a 600 mg dose increased active GLP-1 levels after a standardized meal. Furthermore, LC15-0444 was generally well tolerated without significant side effects.[23] In a phase II study performed in 145 Korean subjects with type 2 diabetes mellitus at doses of 50, 100,

and 200 mg for 12 weeks, LC15-0444 treatment even at a dose of 50 mg per day improved the HbA1c, fasting plasma glucose (FPG) levels, and insulin sensitivity.[24] In addition, a recently performed phase III study conducted in 182 patients with type 2 diabetes mellitus including Korean and Indian populations also showed that 24 weeks of LC15-0444 treatment at a dose of 50 mg per day led to significant reductions in HbA1c and FPG levels.[25] In a metformin add-on trial performed in 425 Asian patients with inadequately controlled type 2 diabetes being treated with metformin alone, gemigliptin showed comparable efficacy and safety profiles to sitagliptin.[26]

In the present study, we observed that the increased urinary excretion of 8-isoprostane after UUO, reflecting the increased oxidative stress in the kidney, was attenuated in mice treated with LC15-0444. However, we did not observe significant differences in plasma 8-isoprostane levels among the four groups. These results suggest that LC15-0444 treatment mainly suppresses renal oxidative stress without systemic antioxidative stress effects. We found significant upregulation of inflammatory molecules in the contralateral unobstructed kidney compared with the sham kidney, and these changes led to increased urinary levels of 8-isoprostane after UUO. We also observed that UUO-induced upregulation of NOX4 after UUO was attenuated in mice treated with
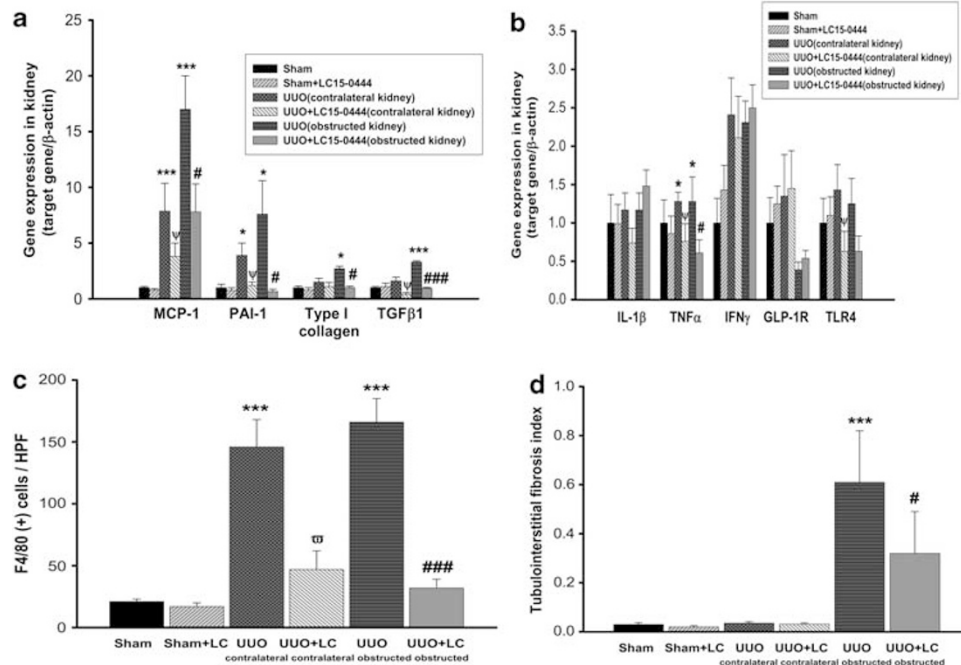
Figure 4 Effects of LC15-0444 (LC) on inflammation and fibrosis in the kidney. (**a**) Effects of LC on the expression of inflammatory and fibrotic molecules. (**b**) Effects of LC on the expression of inflammatory cytokines and the glucagon-like peptide-1 (GLP-1) receptor. (**c**) Effects of LC on macrophage infiltration. (**d**) Effects of LC on tubulointerstitial fibrosis. In this experiment, each sample was run in triplicate, and the corresponding non-reverse transcribed mRNA samples were used as negative controls. The mRNA level of each sample was normalized to that of β-actin mRNA. Data are expressed as mean ± s.e.m.; *$P < 0.05$, ***$P < 0.001$ *vs* sham and sham + LC; #$P < 0.05$, ###$P < 0.001$ *vs* unilateral ureteral obstruction (UUO) (obstructed kidney); $^{\Psi}P < 0.05$, $^{\omega}P < 0.001$ *vs* UUO (contralateral unobstructed kidney). IFNγ, interferon γ; IL-1β, interleukin-1β; MCP-1, monocyte chemoattractant peptide-1; PAI-1, plasminogen activator inhibitor-1; TGFβ1, transforming growth factor-β1; TLR4, toll-like receptor 4; TNF-α, tumor necrosis factor-α.

LC15-0444. These results agree with other research showing that DPPIV inhibition decreases oxidative stress in various organs.[18,27] Taken together, these results suggest that DPPIV inhibition decreases oxidative stress in the kidney, leading to improved renal function.

Our study differs from previous research in that we directly determined DPPIV activity in the kidney rather than simply measuring DPPIV expression. Our model showed that DPPIV activity was increased after UUO and that LC15-0444 treatment suppressed DPPIV activity. Our results suggest that renal DPPIV activation may have a role in the progression of tubulointerstitial fibrosis.

We also found evidence that LC15-0444 improved inflammatory and fibrotic processes, including MCP-1, type I collagen, TGFβ1, and PAI-1 expression, as well as macrophage infiltration. The differing effects of DPPIV inhibition on tissue inflammation may stem from the differences in animal models and individual disease states.[28,29] Taken together, these results suggest that increased macrophage infiltration, TGFβ activation, and downstream Smad2/3 pathway activation may have roles in renal inflammation that are blocked by DPPIV inhibition.

In the present study, we observed that urinary excretion of albumin was markedly suppressed by LC15-0444. Although tubulointerstitial fibrosis was not observed in the contralateral unobstructed kidney compared with obstructed

kidney, we observed that inflammatory changes were significantly evident compared with the control sham group, and LC15-0444 treatment markedly suppressed renal inflammation in the contralateral unobstructed kidney, and these changes led to decreased urinary excretion of albumin. In addition, we also observed that DPPIV activity was suppressed after LC15-0444 treatment in the sham operation group. However, there were no significant increase in urinary albumin excretion, oxidative stress and morphologic alterations in the LC15-0444-treated sham group compared with the control sham group, which suggests an independent effect of LC15-0444.

It has been determined that DPPIV cleaves HMGB1 at its N terminus and markedly reduces HMGB1-induced endothelial cell migration and tubular-like structure formation *in vitro*, as well as vessel formation *in vivo*.[11] HMGB1, a nuclear protein that regulates gene transcription, is passively released after cell injury and has been implicated in tissue inflammation in animal models of kidney injury.[13,30] HMGB1 is a known ligand of TLR, which leads to the activation of NF-κB, ultimately increasing tissue inflammation.[12,31] We also found that renal expression of HMGB1 was decreased in mice given LC15-0444 treatment in this study. Similarly, TLR4 and NF-κB expression was increased in obstructed kidneys and decreased in mice treated with LC15-0444. Considering that HMGB1 can be
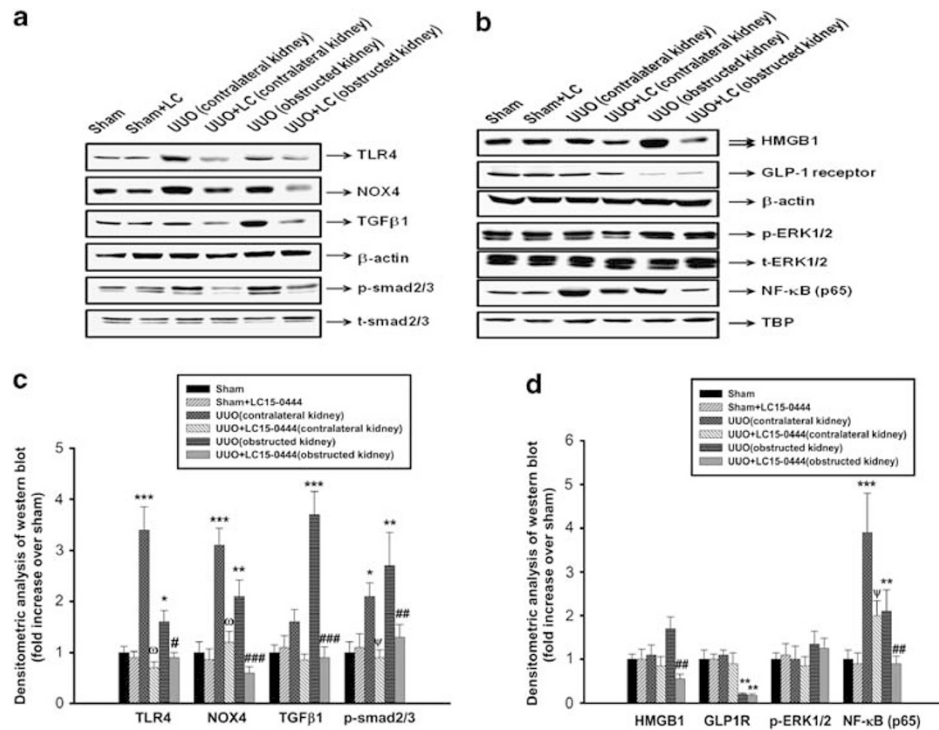
Figure 5 Effects of LC15-0444 (LC) on the expression of fibrotic and inflammatory molecules in the renal cortical tissues in experimental animals. (**a**, **b**) Representative western blots of TLR4, NOX4, TGFβ1, phosphorylated (p)-Smad2/3, HMGB1, GLP-1 receptor, p-ERK1/2 and NF-κB (p65) in the kidney. (**c**, **d**) Densitometric analysis of western blot results. Data are shown as mean ± s.e.m.; *$P < 0.05$, **$P < 0.01$, ***$P < 0.001$ vs sham and sham + LC; #$P < 0.05$, ##$P < 0.01$, ###$P < 0.001$ vs unilateral ureteral obstruction (UUO) (obstructed kidney); $^{\Psi}P < 0.05$, $^{\omega}P < 0.001$ vs UUO (contralateral unobstructed kidney). GLP-1R, glucagon-like peptide-1 receptor; HMGB1, high-mobility group box-1; NF-κB, nuclear factor-κB; NOX4, NADPH oxidase 4; TGFβ1, transforming growth factor-β1; TLR4, toll-like receptor 4; TBP, TATA-binding protein.
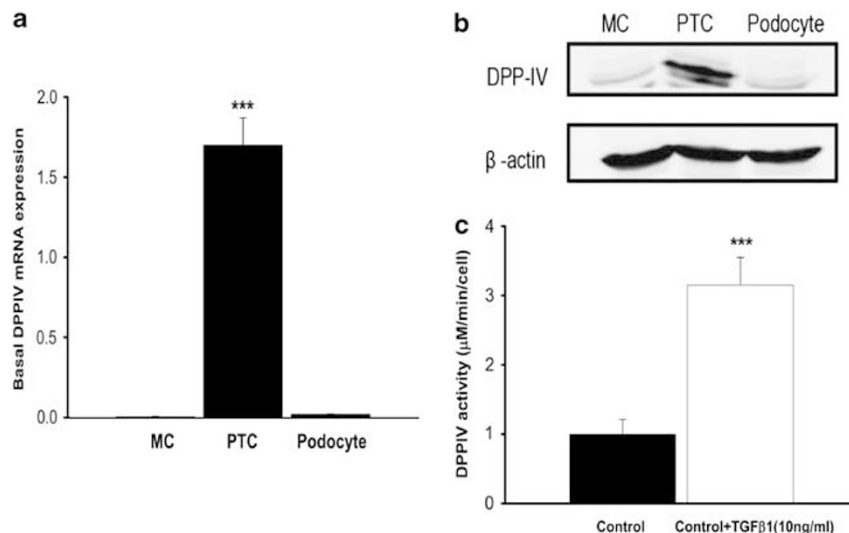

Figure 6 Dipeptidyl peptidase IV (DPPIV) expression in renal cells and effect of transforming growth factor-β1 (TGFβ1) on DPPIV activity in proximal tubule cells. (**a**) Basal DPPIV mRNA expression in various renal cells. (**b**) Basal DPPIV protein expression in various renal cells. (**c**) Effects of TGFβ1 stimulation on DPPIV activity in proximal tubule cells. Data are shown as mean ± s.e.m.; ***$P < 0.001$ vs MC and podocyte or control. MC, mesangial cell; PTC, proximal tubule cell.

released into the extracellular space from damaged proximal tubule cells or infiltrating activated macrophages,[11,12] it is possible that LC15-0444 treatment reduces macrophage infiltration in proximal tubule cells and suppresses HMGB1 expression in the kidney. The role of HMGB1 in tubulointerstitial fibrosis merits further study.

In this study, we observed that basal DPPIV activity was highest in proximal tubule cells compared to mesangial cells or podocytes. For these reasons, we tested whether TGFβ1 stimulation increased DPPIV activity because TGFβ1 is a well-known central player in renal fibrosis in the UUO model.[32,33] Interestingly, we found that exogenous administration of TGFβ1 markedly enhanced DPPIV activity in proximal tubule cells. These results are in contrast with those from a previous study using human peritoneal mesothelial cells and human dermal fibroblasts, which shows that exogenous TGFβ1 decreases DPPIV activity.[34,35] These different results may be because of differences in experimental cells and currently there is no data on the effect of TGFβ1 on DPPIV activity in renal cells. Taken together, these results suggest that DPPIV activation may contribute to the progression of renal disease.

In the present study, we observed increased inflammation in the contralateral kidney after UUO. There are several possible mechanisms responsible for increased inflammation in the contralateral kidney as well as in the obstructed kidney. The contralateral unobstructed kidney may undergo hyperfiltration state to compensate for the decreased renal unit, and the activation of renin–angiotensin system (RAS) from obstructed kidney may induce systemic RAS activation. Consequently, contralateral kidney is exposed to increasing levels of circulating angiotensin II.[36] There is a great deal of evidence implicating that hyperfiltration is associated with increased renal tissue inflammation in experimental animal models.[37,38] Our result were in line with recent report that oxidative stress and inflammation is increased in the contralateral kidney after chronic UUO in the neonatal mice.[39]

In conclusion, our results suggest that DPPIV inhibition protects against renal injury in mice via several mechanisms related to fibrosis, inflammation, and oxidative damage, independently of its hypoglycemic effects. We recommend further study of DPPIV inhibitors as treatments of progressive renal disease.

DISCLOSURE/CONFLICT OF INTEREST
The authors declare no conflict of interest.

1. Panchapakesan U, Mather A, Pollock C. Role of GLP-1 and DPP-4 in diabetic nephropathy and cardiovascular disease. Clin Sci 2013;124: 17–26.
2. Simsek S, de Galan BE. Cardiovascular protective properties of incretin-based therapies in type 2 diabetes. Curr Opin Lipidol 2012;23:540–547.
3. Drucker DJ, Nauck MA. The incretin system: glucagon-like peptide-1 receptor agonists and dipeptidyl peptidase-4 inhibitors in type 2 diabetes. Lancet 2006;368:1696–1705.
4. Jeffery CJ. Moonlighting proteins. Trends Biochem Sci 1999;24:8–11.
5. Ejiri S. Moonlighting functions of polypeptide elongation factor 1: from actin bundling to zinc finger protein R1-associated nuclear localization. Biosci Biotechnol Biochem 2002;66:1–21.
6. Boonacker E, Van Noorden CJ. The multifunctional or moonlighting protein CD26/DPPIV. Eur J Cell Biol 2003;82:53–73.
7. Mentlein R. Dipeptidyl-peptidase IV (CD26)—role in the inactivation of regulatory peptides. Regul Pept 1999;85:9–24.
8. Hocher B, Reichetzeder C, Alter ML. Renal and cardiac effects of DPP4 inhibitors—from preclinical development to clinical research. Kidney Blood Press Res 2012;36:65–84.
9. Proost P, Struyf S, Couvreur M, et al. Post-translational modifications affect the activity of the human monocyte chemotactic proteins MCP-1 and MCP-2: identification of MCP-2(6–76) as a natural chemokine inhibitor. J Immunol 1998;160:4034–4041.
10. Heymann E, Mentlein R. Liver dipeptidyl aminopeptidase IV hydrolyzes substance P. FEBS Lett 1978;91:360–364.
11. Marchetti C, Di Carlo A, Facchiano F, et al. High mobility group box 1 is a novel substrate of dipeptidyl peptidase-IV. Diabetologia 2012; 55:236–244.
12. Lotze MT, Tracey KJ. High-mobility group box 1 protein (HMGB1): nuclear weapon in the immune arsenal. Nat Rev Immunol 2005;5: 331–342.
13. Penfold SA, Coughlan MT, Patel SK, et al. Circulating high-molecular-weight RAGE ligands activate pathways implicated in the development of diabetic nephropathy. Kidney Int 2010;78:287–295.
14. Tiruppathi C, Miyamoto Y, Ganapathy V, et al. Hydrolysis and transport of proline-containing peptides in renal brush-border membrane vesicles from dipeptidyl peptidase IV-positive and dipeptidyl peptidase IV-negative rat strains. J Biol Chem 1990;265:1476–1483.
15. Tinoco AD, Tagore DM, Saghatelian A. Expanding the dipeptidyl peptidase 4-regulated peptidome via an optimized peptidomics platform. J Am Chem Soc 2010;132:3819–3830.
16. Bonegio RG, Fuhro R, Wang Z, et al. Rapamycin ameliorates proteinuria associated tubulointerstitial fibrosis inflammation and fibrosis in experimental membranous nephropathy. J Am Soc Nephrol 2005;16:2063–2072.
17. Lim KS, Cho JY, Kim BH, et al. Pharmacokinetics and pharmacodynamics of LC15-0444, a novel dipeptidyl peptidase IV inhibitor, after multiple dosing in healthy volunteers. Br J Clin Pharmacol 2009;68:883–890.
18. Mega C, de Lemos ET, Vala H, et al. Diabetic nephropathy amelioration by a low-dose sitagliptin in an animal model of type 2 diabetes (Zucker diabetic fatty rat). Exp Diabetes Res 2011;2011:1–12.
19. Glorie LL, Verhulst A, Matheeussen V, et al. DPP4 inhibition improves functional outcome after renal ischemia–reperfusion injury. Am J Physiol Renal Physiol 2012;303:F681–F688.
20. Liu WJ, Xie SH, Liu YN, et al. Dipeptidyl peptidase IV inhibitor attenuates kidney injury in streptozotocin-induced diabetic rats. J Pharmacol Exp Ther 2012;340:248–255.
21. Chaykovska L, von Websky K, Rahnenführer J, et al. Effects of DPP-4 inhibitors on the heart in a rat model of uremic cardiomyopathy. PLoS One 2011;6:e27861.
22. Kim D, Wang L, Beconi M, et al. (2R)-4-oxo-4-[3-(trifluoromethyl)-5,6-dihydro[1,2,4]triazolo[4,3-a] pyrazin-7(8H)-yl]-1-(2,4,5-trifluorophenyl) butan-2-amine: a potent, orally active dipeptidyl peptidase IV inhibitor for the treatment of type 2 diabetes. J Med Chem 2005;48: 141–151.
23. Lim KS, Kim JR, Choi YJ, et al. Pharmacokinetics, pharmacodynamics, and tolerability of the dipeptidyl peptidase IV inhibitor LC15-0444 in healthy Korean men: a doseblock-randomized, double-blind, placebo-controlled, ascending single-dose, phase I study. Clin Ther 2008;30: 1817–1830.
24. Rhee EJ, Lee WY, Yoon KH, et al. A multicenter, randomized, placebo-controlled, double-blind phase II trial evaluating the optimal dose, efficacy and safety of LC 15-0444 in patients with type 2 diabetes. Diabetes Obes Metab 2010;12:1113–1119.
25. Yang SJ, Min KW, Gupta SK, et al. A multicentre, multinational, randomized, placebo-controlled, double-blind, phase 3 trial to evaluate the efficacy and safety of gemigliptin (LC15-0444) in patients with type 2 diabetes. Diabetes Obes Metab 2013;15:410–416.
26. Rhee EJ, Lee WY, Min KW, et al. Gemigliptin Study 006 Group. Efficacy and safety of the dipeptidyl peptidase-4 inhibitor gemigliptin

compared with sitagliptin added to ongoing metformin therapy in patients with type 2 diabetes inadequately controlled with metformin alone. Diabetes Obes Metab 2013;15:523–530.

27. Rizzo MR, Barbieri M, Marfella R, *et al*. Reduction of oxidative stress and inflammation by blunting daily acute glucose fluctuations in patients with type 2 diabetes: role of dipeptidyl peptidase-IV inhibition. Diabetes Care 2012;35:2076–2082.

28. Busso N, Wagtmann N, Herling C, *et al*. Circulating CD26 is negatively associated with inflammation in human and experimental arthritis. Am J Pathol 2005;166:433–442.

29. Ning XH, Ge XF, Cui Y, *et al*. Ulinastatin inhibits unilateral ureteral obstruction-induced renal interstitial fibrosis in rats via transforming growth factor β (TGF-β)/Smad signalling pathways. Int Immunopharmacol 2013;15:406–413.

30. Shinosaki T, Kobayashi T, Kimura K, *et al*. Involvement of dipeptidyl peptidase IV in immune complex-mediated glomerulonephritis. Lab Invest 2002;82:505–513.

31. Wu H, Ma J, Wang P, *et al*. HMGB1 contributes to kidney ischemia reperfusion injury. J Am Soc Nephrol 2010;21:1878–1890.

32. Wright EJ, McCaffrey TA, Robertson AP, *et al*. Chronic unilateral ureteral obstruction is associated with interstitial fibrosis and tubular expression of transforming growth factor-beta. Lab Invest 1996; 74:528–537.

33. Vaughan Jr ED, Marion D, Poppas DP, *et al*. Pathophysiology of unilateral ureteral obstruction: studies from Charlottesville to New York. J Urol 2004;172:2563–2569.

34. Kajiyama H, Shibata K, Ino K, *et al*. Possible involvement of SDF-1alpha/CXCR4-DPPIV axis in TGF-beta1-induced enhancement of migratory potential in human peritoneal mesothelial cells. Cell Tissue Res 2007;330:221–229.

35. Sorrell JM, Brinon L, Baber MA, *et al*. Cytokines and glucocorticoids differentially regulate APN/CD13 and DPPIV/CD26 enzyme activities in cultured human dermal fibroblasts. Arch Dermatol Res 2003;295:160–168.

36. Frøkiaer J, Knudsen L, Nielsen AS, *et al*. Enhanced intrarenal angiotensin II generation in response to obstruction of the pig ureter. Am J Physiol 1992;263:F527–F533.

37. Sasaki M, Shikata K, Okada S, *et al*. The macrophage is a key factor in renal injuries caused by glomerular hyperfiltration. Acta Med Okayama 2011;65:81–89.

38. Vaziri ND, Bai Y, Ni Z, *et al*. Intra-renal angiotensin II/AT1 receptor, oxidative stress, inflammation, and progressive injury in renal mass reduction. J Pharmacol Exp Ther 2007;323:85–93.

39. Forbes MS, Thornhill BA, Galarreta CI, *et al*. Chronic unilateral ureteral obstruction in the neonatal mouse delays maturation of both kidneys and leads to late formation of atubular glomeruli. Am J Physiol Renal Physiol 2013;305:F1736–F1746.